Microb Health Dis 2023; 5 (1): e826

MSH2 AND *APC* MUTATED MOUSE MODELS CLOSELY MIMIC THE DIFFERENCES BETWEEN HEREDITARY NONPOLYPOSIS COLORECTAL CANCER AND FAMILIAL ADENOMATOUS POLYPOSIS

B. Oliveira Rocha[1,2,3], H. Xavier-Ferreira[2,3], A. Vilarinho[2,3,4], B. Cavadas[2,3], I. Gullo[2,3,5,6], C. Resende[2,3]

[1]Faculty of Medicine of the University of Porto (FMUP), Porto, Portugal
[2]Instituto de Investigação e Inovação em Saúde (i3S), University of Porto, Porto, Portugal
[3]Institute of Molecular Pathology and Immunology, University of Porto (Ipatimup), Porto, Portugal
[4]Institute of Biomedical Sciences Abel Salazar (ICBAS), Porto, Portugal
[5]Department of Pathology, Centro Hospitalar Universitário de São João (CHUSJ), Porto, Portugal
[6]Department of Pathology, Faculty of Medicine of the University of Porto (FMUP), Porto, Portugal

Corresponding Author: Carlos Alberto Resende, Ph.D; e-mail: cresende@ipatimup.pt

Abstract – ***Introduction:*** Hereditary colorectal cancer occurs mainly in the setting of hereditary nonpolyposis colorectal cancer and familial adenomatous polyposis. *VCMsh2*$^{LoxP/LoxP}$ and *Apc*$^{Min/+}$ are mouse models of these two human syndromes. The goal of this study was to evaluate whether these two models recapitulate the differences observed between hereditary nonpolyposis colorectal cancer and familial adenomatous polyposis.

Materials and Methods: Animals were characterized and compared regarding time to disease manifestation and tumor incidence. Tumors were characterized regarding histopathologic features, immune infiltrate as evaluated by immunohistochemistry, and mutation burden through whole-exome sequencing.

Results: *VCMsh2*$^{LoxP/LoxP}$ mice showed a longer average lifespan (367.9 days) comparatively to *Apc*$^{Min/+}$ mice (135.4 days). *Apc*$^{Min/+}$ mice showed a higher average incidence of intestinal tumors per animal (58.9) comparatively to *VCMsh2*$^{LoxP/LoxP}$ mice (3.54). The immune infiltrate was overall higher in *VCMsh2*$^{LoxP/LoxP}$ tumors, with a significant difference for CD8+ T cells. The mean number of somatic genetic variants was significantly higher in tumors from *VCMsh2*$^{LoxP/LoxP}$ than in *Apc*$^{Min/+}$ mice.

Conclusions: Results obtained with these preclinical mouse models are comparable and translatable to the respective human scenario, demonstrating they are appropriate models to study and compare different models of intestinal tumorigenesis. These models are central to our understanding of colorectal tumorigenesis, including the role of microbiota in such processes.

Keywords: Gastrointestinal cancer, Cancer genetics, Hereditary intestinal cancer, Tumor infiltrating lymphocytes, Preclinical mouse models.

INTRODUCTION

Colorectal cancer (CRC) is one of the most common neoplasias in the world as well as a leading cause of cancer-related death[1,2]. Classically, its onset and development have been attributed to two principal pathways of tumorigenesis: chromosomal and microsatellite instability pathways[3,4]. Regardless of which pathway is involved, mutations in tumor suppressor genes and/or oncogenes occur in the intestinal epithelial cells, which will confer them an advantage in proliferation and/or survival[5-7]. From an etiopathogenic standpoint, colorectal cancer can be classified as: I) sporadic, accounting for about 70% of cases; II) with familial predisposition, which accounts for about 10-30%; and III) hereditary, which accounts for the remaining 5-7% of cases[5]. There are different inherited disorders associated with colorectal cancer, the most frequent being Hereditary Nonpolyposis Colorectal Cancer (HNPCC, also known as Lynch Syndrome) and Familial Adenomatous Polyposis (FAP)[5,8].

HNPCC is the most frequent hereditary form of colorectal cancer[4,9-13]. It is caused by germline variants in genes codifying proteins involved in the process of DNA mismatch repair (MMR), namely MLH1, PMS2, MSH2 and MSH6[13-15]. *MLH1* and *MSH2* are the germline variants most frequently associated with an increased risk of colorectal cancer[14,16-18], with a cumulative incidence by the age of 75 years of 46% and 43%, respectively[13,19]. Due to the impairment of DNA mismatch repair, the accumulation of mutations in microsatellite regions leads to the alteration of microsatellite fragment size, i.e., microsatellite instability (MSI)[20]. Moreover, DNA mismatch repair impairment will also increase the tumor mutation burden[20].

FAP is the second most frequent hereditary form of colorectal cancer[4,9,13]. It is an autosomal dominant disorder resulting from a germline mutation in the adenomatous polyposis gene (*APC*)[13,19,21-23]. *APC* gene mutations occur in about 80-90% of cases[19]. However, in the remaining percentage of patients, other mutations can be found, such as the biallelic mutation of the *MUTYH* gene, associated with recessive hereditary polyposis[13,21]. The APC protein exerts a negative regulation on the Wnt signaling pathway, which is associated with intestinal epithelium homeostasis[24,25]. Loss of APC function leading to Wnt signaling pathway activation will deregulate the balance between cell proliferation and differentiation and thus ultimately result in the development of multiple adenomas[24,26].

Understanding neoplasia depends on the identification of the biological role of mutated genes involved in the process of tumorigenesis. Mice carrying mutations in relevant genes represent very useful models for tumorigenesis studies[27-29]. The two mouse models we used in our study, *VCMsh2*$^{LoxP/LoxP}$ and *Apc*$^{Min/+}$, are widely used preclinical representatives of intestinal tumorigenesis. The *VCMsh2*$^{LoxP/LoxP}$ mouse is a model to study the MSI pathway in intestinal neoplasia, since it allows for an intestinal epithelium-specific deletion of the *Msh2* gene[14]. In these mice the expression of Cre recombinase under the activation of *Villin* promoter (Villin-Cre, acronym VC) occurs in the villus and crypt epithelial cells of the small intestine and colon, allowing a tissue-specific deletion of the *Msh2* gene when the two alleles of this gene are flanked by LoxP sites[30]. Therefore, the *VCMsh2*$^{LoxP/LoxP}$ mice stands as a valuable preclinical model to study, allowing to establish a correlation to human HNPCC[14]. The *Apc*$^{Min/+}$ model was first developed in 1990[27], and is associated with the development of multiple neoplasias in the intestine[27,31], due to the presence of a spontaneous germline mutation in the tumor suppressor gene *Apc*[31]. These mice are viable only if heterozygotic for the substitution T>A in codon 850, which gives rise to a nonsense mutation, translating in a stop codon and thus truncating the full-length protein[31]. *APC* is a frequently mutated gene in human colorectal cancer, being also the genetic cause for FAP[31]. Thus, *Apc*$^{Min/+}$ mice are a useful model to study intestinal cancer[27,31], having the potential to establish connection with this human disease.

With this study, we aim to evaluate whether these two mice models recapitulate the characteristics observed in HNPCC and FAP. Specific objectives encompass the analysis of several clinicopathological characteristics, including age at disease presentation, incidence of intestinal tumors, histological classification, mutation burden and tumor lymphocyte infiltrate.

MATERIALS AND METHODS

Mouse Models

All mice were housed in the Animal Facility of Instituto de Investigação e Inovação em Saúde (i3S, University of Porto) and all procedures were performed according to the Ethics Committee and Direção Geral de Alimentação e Veterinária (DGAV) guidelines for care and use of laboratory animals. *VCMsh2*$^{LoxP/LoxP}$ and *Apc*$^{Min/+}$ (both in house) were housed in a pathogen-free and light-controlled environment, fed standard chow, and allowed water and food *ad libitum*.

Tissue Collection and Preservation

Euthanasia was performed as soon as mice exhibited irreversible signs of disease manifestation, such as weight loss (>20% initial body weight), anemia and bloody stools. Mice were anesthetized with isoflurane before euthanasia and then euthanized by cervical dislocation. After euthanasia, the gastrointestinal tube was removed, and the dissection of the small intestine (divided in three portions: proximal, intermediate and distal) and colon was performed. Each portion of the small intestine and colon was cleaned with fresh saline solution (0.9% NaCl), distended in a solid support and sequentially opened longitudinally. The identification of tumors was macroscopically assessed, and their number, size and anatomical location recorded. Tumor size was determined using a digital caliper. From the identified tumors, some were isolated and preserved in 10% formalin, as well as portions of normal tissue. For the *Apc*$^{Min/+}$ mice, swiss-rolls of portions of the small intestine were also performed, due to the high number of tumors, and preserved in 10% formalin for 24 hours. Thereafter, the formalin-fixed tissues were paraffin-embedded to originate formalin fixed paraffin-embedded (FFPE) blocks.

Whole-Exome Sequencing

DNA was extracted from tumors (4 tumors from *VCMsh2*$^{LoxP/LoxP}$ and 4 tumors from *Apc*$^{Min/+}$) using the MagMax Kit (Thermo Fisher Scientific). DNA was also extracted from ear skin (1 case from *VCMsh2*$^{LoxP/LoxP}$ and 1 case from *Apc*$^{Min/+}$), for whole-exome sequencing data normalization, allowing the removal of all constitutional variants. DNA concentration was determined with Qubit 2.0 Fluorometer (Invitrogen), using the High-Sensitivity DNA quantification protocol. DNA from tumors and normal samples was prepared for exome capture and DNA library preparation using the SureSelect XT Mouse All Exon Kit (Agilent). DNA libraries were sequenced using the NovaSeq6000 System (Illumina). Exomes were sequenced to 100x average read depth.

Exome analysis started with the quality control (QC) of the raw data, in FASTQ format, to detect low quality bases, abnormal GC content and adapter contamination that needed to be addressed before alignment. After QC analysis, reads were mapped to the mouse reference genome GRCm38, using the Burrows-Wheeler Aligner (BWA) software package with the "mem" option with default parameters. Aligned sequencing data from BWA, in SAM (Sequence Alignment/Map) format, were converted into binary format and sorted with SAMtools. After sorting, PCR and optical duplicates were marked with Biobambam2. By marking these duplicates, potential bias of variant calling algorithms was mitigated. After marking duplication, GATK Base Quality Score Recalibration (BQSR) was applied. After BQSR, files were ready for somatic mutation analysis. Quality control of the alignment was carried by bamdst which displays the percentage of mapped reads, percentage of covered exons and genome coverage.

Somatic mutations were called using the generated alignment files from the tumor and the corresponding normal skin tissue. Somatic variant calling was carried by the SomaticSeq ensemble approach. SomaticSeq combines eight state-of-the-art somatic mutation callers for single nucleotide polymorphisms (SNP) and insertion-deletion (indels) mutations: MuTect, VarScan2, JointSNVMix2, SomaticSniper, VarDict, Muse, LoFreq and Strelka2. Only variants

identified in at least half of the callers were considered for downstream analysis. Features such as strand bias, read counts, mapping quality and base call quality were also considered to achieve a high-confidence call set.

Immunohistochemistry

Serial 4 µm tissue sections were prepared from all FFPEs blocks. Hematoxylin and eosin staining was performed for histopathological analysis. Immunohistochemistry (IHC) was performed with antibodies against murine CD3 (ab5690, Abcam), CD4 (ab183685, Abcam), and CD8 (ab209775, Abcam). IHC was started by dissolving the paraffin in xylene and hydrating the tissues in successive rounds of decreasing concentration alcohol solutions, being the last round running water. The slides were then ready for antigen retrieval in buffers previously optimized for each antibody (CD3 – EDTA buffer, pH8; CD4 – citrate-based buffer, pH6; CD8 – Tris/EDTA buffer, ph9), for 35 minutes in a vaporizer (at ~99°C). The slides were then left to reach room temperature. Between a series of washes in PBS Tween 0.1%, the tissues were placed in a solution of 3% hydrogen peroxide (Merck) and methanol (Merck) in order to inactivate endogenous peroxidase. Afterwards, tissue slides were treated with Ultravision Protein Block solution (Thermo Fisher Scientific), followed by primary antibody incubation at 4°C overnight. The dilution of each antibody used was as follows: CD3 - 1:200; CD4 - 1:200; CD8 - 1:2000. After washing steps with PBS Tween 0.1%, secondary antibody (EnVision Detection Systems Peroxidase/DAB, Rabbit/Mouse, Dako) incubation was performed, followed by DAB staining (Dako). After placing the slides in hematoxylin, they were subjected to rounds of gradual and sequential dehydration and mounted with DPX mounting medium (Merck).

Image Analysis and Cell Counting

CD3+, CD4+ and CD8+ cells were counted in order to compare the densities of the different immune cell types infiltrating the murine tumors. For each lesion, a minimum of 4 non-overlapping fields at 200x magnification were collected with Axioskop 2 microscope (Zeiss). After image collection, positive cells were manually counted using the Cell Counter plugin of Image J software [National Institutes of Health, Bethesda, MD, USA and the Laboratory for Optical and Computational Instrumentation (LOCI), University of Wisconsin, Madison, WS, USA]. The number of positive cells per image was recorded.

Statistical Analysis

Comparisons between two experimental groups were performed using GraphPad Prism 6,0 (GraphPad Software, San Diego, CA, USA). All tests were two-sided, and differences were considered significant when $p < 0.05$. Comparisons of categorical variables were performed using a Fischer's exact test. Comparisons of quantitative variables were performed using non-parametric Mann–Whitney *U*-test, when data did not show a normal distribution, or using a parametric t-test, when data exhibited a distribution statistically close to normality.

RESULTS

Table 1 summarizes the comparison of different biological parameters between the $Apc^{Min/+}$ and $VCMsh2^{LoxP/LoxP}$ mouse models, namely age at euthanasia, tumor size and tumor multiplicity. Due to the rapid onset and severity of symptoms of intestinal tumors, mice were euthanized at the age where manifestation of disease occurred. $VCMsh2^{LoxP/LoxP}$ mice showed a significantly longer lifespan, with an average of 367.9 days, comparatively to $Apc^{Min/+}$ mice which showed an average lifespan of 135.4 days ($p < 0.001$). Moreover, looking at tumor size, $VCMsh2^{LoxP/LoxP}$ showed tumors with a significantly bigger average size comparatively to $Apc^{Min/+}$ tumors ($p < 0.001$). As for tumor multiplicity, $Apc^{Min/+}$ mice had a significantly higher

TABLE 1. COMPARISON OF AGE OF EUTHANASIA, TUMOR INCIDENCE, SIZE AND MULTIPLICITY BETWEEN *VCMSH2*$^{LOXP/LOXP}$ AND *APC*$^{MIN/+}$ MICE.

Genotype	N	Age (days) mean ± SD	*p*	Tumor size (mm^2) mean ± SD	Tumor multiplicity mean ± SD	*p*
VCMsh2$^{LoxP/LoxP}$	11	367.9 ± 40.6		33.7 ± 5.5	3.5 ± 0.6	
			< 0.001			< 0.001
Apc$^{Min/+}$	9	135.4 ± 58.9		4.3 ± 0.2	58.9 ± 15.4	

N, number of mice studied; Age, time from birth to euthanasia; SD, standard deviation; SEM, standard error mean. For *VCMsh2*$^{LoxP/LoxP}$ euthanasia was performed after disease manifestation or at 55 weeks old; *Apc*$^{Min/+}$ mice were euthanized at disease manifestation.

number of intestinal tumors, with an average of 58.9 per animal, comparatively to *VCMsh-2*$^{LoxP/LoxP}$ mice whose average is 3.5 per animal ($p < 0.001$) (Table 1). Histopathological analysis revealed adenomas with low and high-grade dysplasia in *Apc*$^{Min/+}$ mice, while half of the tumors from *VCMsh2*$^{LoxP/LoxP}$ mice were adenocarcinomas. This difference in tumors histopathology between *Apc*$^{Min/+}$ and *VCMsh2*$^{LoxP/LoxP}$ is statistically different ($p < 0.001$) (Figure 1).

In order to determine the tumor mutation burden, we quantified the number of coding variants through whole-exome sequencing (WES) of intestinal tumors from *VCMsh2*$^{LoxP/LoxP}$ (n=4) and *Apc*$^{Min/+}$ (n=4) mice. Data normalization was obtained by comparing WES data between tumors and normal skin of model-specific mice. This allowed to eliminate constitutive variants and select only tumor-specific somatic variants. As expected, the average number of somatic variants observed in *VCMsh2*$^{LoxP/LoxP}$ tumors was significantly higher comparatively to *Apc*$^{Min/+}$ tumors ($p = 0.016$), with approximately 10x more variants (Figure 2A). Noteworthy, despite the fact that *VCMsh2*$^{LoxP/LoxP}$ tumors had higher number of somatic variants, the profile of synonymous (S), non-synonymous (NS) and frameshift (F) mutations was similar between the two mouse models, with non-synonymous variants being the most frequent type of tumor-specific variants (Figure 2B).

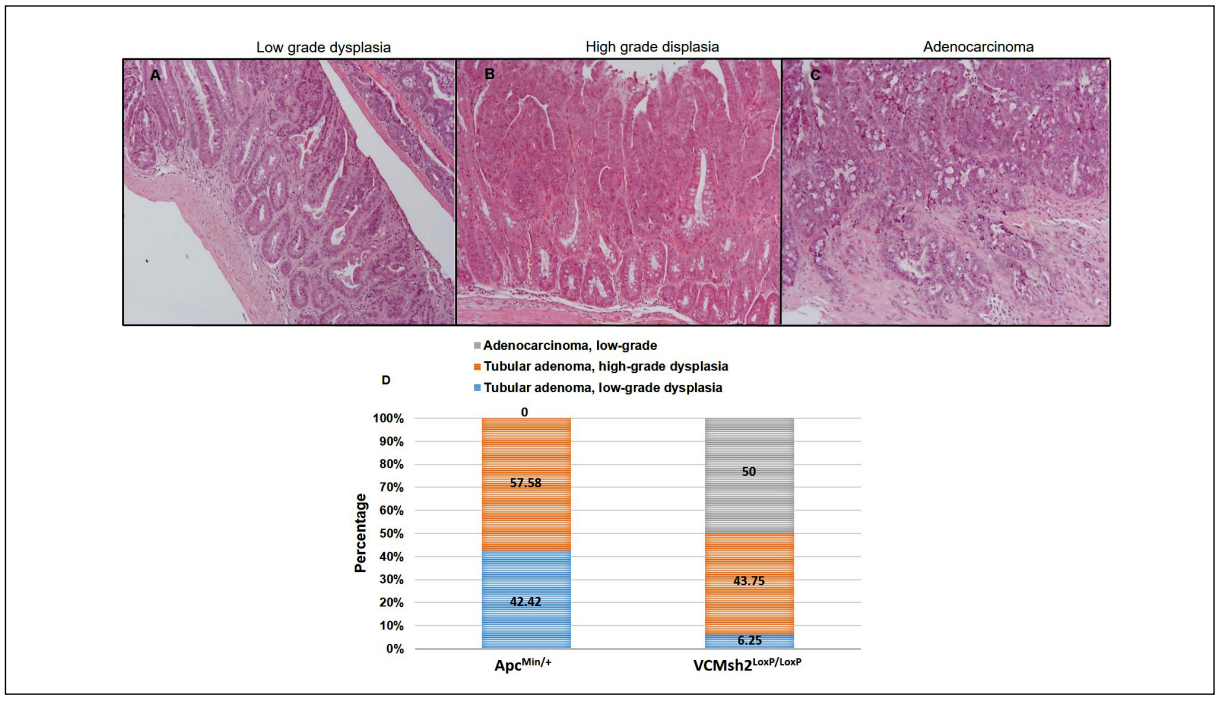

Figure 1. Histological classification of tumors from *Apc*$^{Min/+}$ and *VCMsh2*$^{LoxP/LoxP}$ mice. Representative images at magnification of 100x of: **A,** low grade dysplasia; **B,** high grade dysplasia; and **C,** adenocarcinoma are shown. In D) it is depicted a graphical representation of the percentage of each tumor type from our cohort of *Apc*$^{Min/+}$ and *VCMsh2*$^{LoxP/LoxP}$ mice.

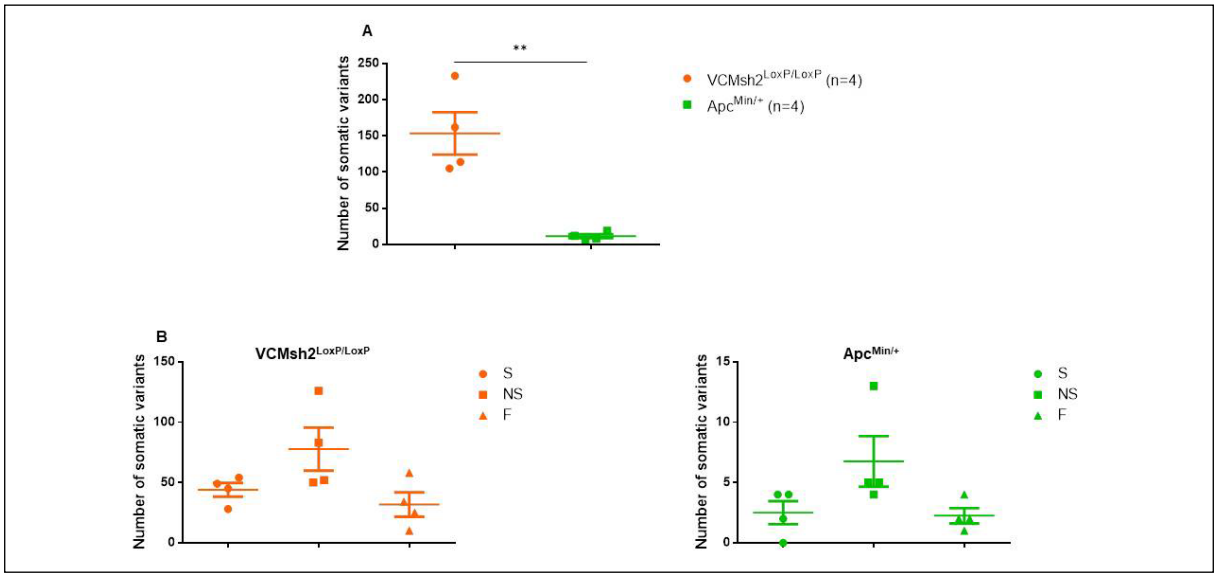

Figure 2. Genomic analyses of intestinal tumors from *VCMsh2*$^{LoxP/LoxP}$ and *Apc*$^{Min/+}$ mice. **A,** Comparison of the number of exon-specific somatic variants. In **B,** the total number of exon-specific variants was divided according to the type of mutation: synonymous (S), non-synonymous (NS) and frameshift (F). $^{**}p < 0.01$. Each dot in the graphics represents a singular tumor and bars represent mean ± SEM.

The last parameter evaluated was immune infiltration, namely by T lymphocytes. We performed immunohistochemistry for CD3 to quantify tumor-infiltrating T lymphocytes, for CD4 to identify helper T lymphocytes and for CD8 to identify cytotoxic T lymphocytes. No statistically significant differences were obtained for the comparison of CD3+ and CD4+ T cells between *VCMsh2*$^{LoxP/LoxP}$ and *Apc*$^{Min/+}$ mice (Figure 3B, C). However, we observed that *VCMsh-2*$^{LoxP/LoxP}$ tumors have a significant increase in the number of infiltrating CD8$^+$ cells ($p = 0.043$) (Figure 3D). These results showed a concordance with human tumor analysis, in which MSI-high tumors have, on average, a higher number of infiltrating T lymphocytes, especially CD8$^+$ cytotoxic T lymphocytes.

DISCUSSION

In the present study we found that *VCMsh2*$^{LoxP/LoxP}$ mice showed a significant larger lifespan, comparatively to *Apc*$^{Min/+}$ mice. Since the mice were euthanized at the manifestation of irreversible signs of disease, we used the mice's lifespan as a surrogate for age at diagnosis. Our findings are in accordance to what is seen in human diseases, with CRC developing earlier in patients with FAP, at an average age of 39 years[24,32], when compared to patients with HNPCC, where the average age at diagnosis varies between 45 and 50 years[24]. Therefore, the results obtained with the murine models show a strong correlation with known clinical human data.

As for tumor multiplicity, we observed that *Apc*$^{Min/+}$ mice have a significant higher number of intestinal tumors, comparatively to *VCMsh2*$^{LoxP/LoxP}$ mice. This difference is also in accordance to what is observed in human diseases, since the number of adenomas in FAP patients can reach hundreds per patient[24]. Noteworthy, histopathological evaluation revealed that tumors from *Apc*$^{Min/+}$ mice were adenomas, establishing once again a correlation with FAP patients. On the other hand, we observed that half of the tumors from *VCMsh2*$^{LoxP/LoxP}$ mice were adenocarcinomas. The significant difference in tumor histology between the two mouse models may, at least partially, result from the different age of manifestation of disease, allowing more time for adenoma progression towards adenocarcinoma in *VCMsh2*$^{LoxP/LoxP}$ mice.

In terms of tumor mutation burden, it is known that due to the impairment of DNA mismatch repair in MSI tumors, the somatic mutations tend to accumulate over time with consequent increase in mutation burden[20]. This is in contrast to MSS tumors, which have a relatively lower

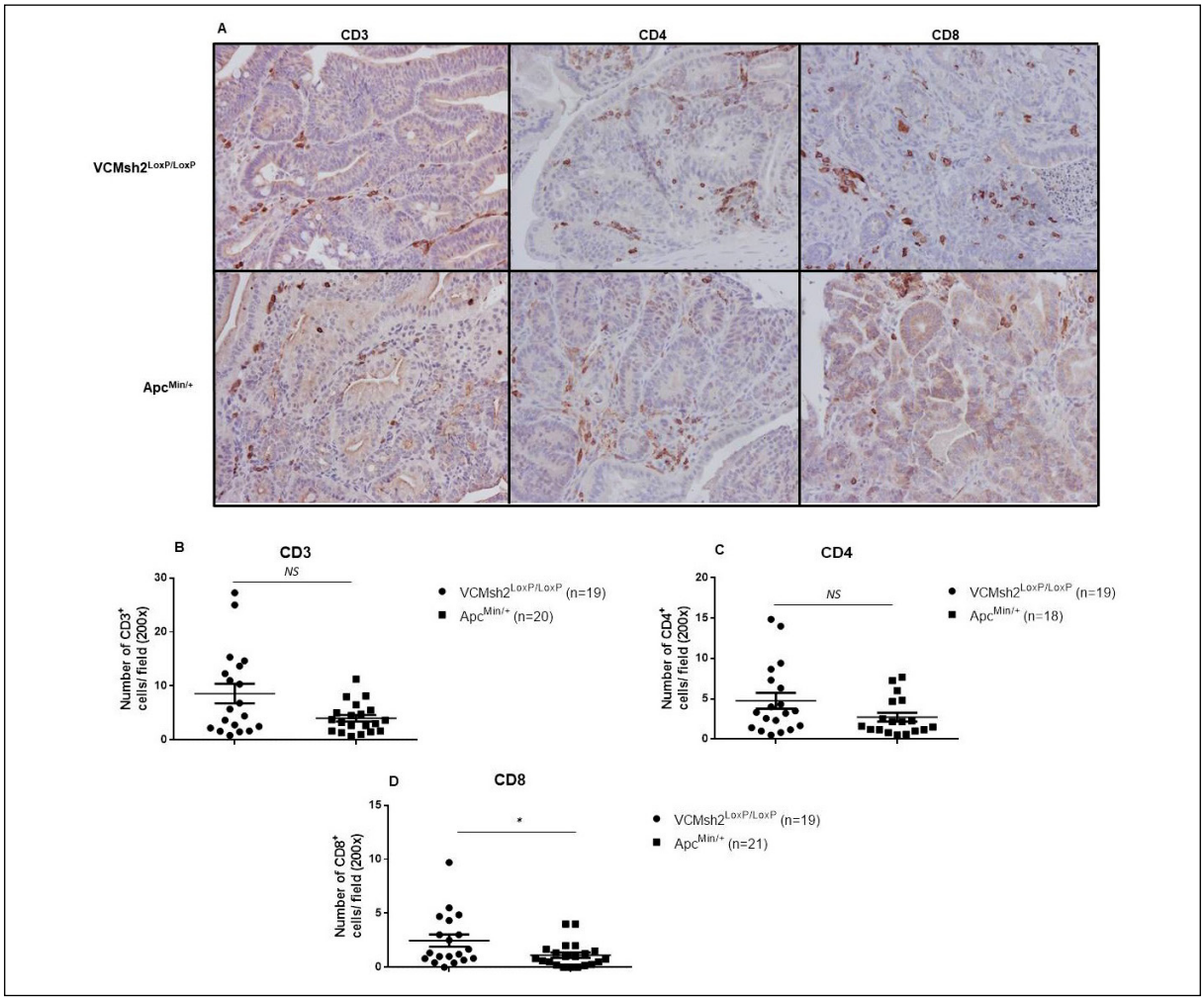

Figure 3. Quantification of infiltrating T lymphocytes in tumors from *Apc*$^{Min/+}$ and *VCMsh2*$^{LoxP/LoxP}$. **A,** Here are shown representative images at magnification of 200x of immunohistochemistry for CD3$^+$, CD4$^+$ and CD8$^+$ in tumors from both mouse models. In **B, C** and **D,** are the graphical representations of the comparison of the number of: B) CD3$^+$; C) CD4$^+$; and D) CD8$^+$ lymphocytes. NS – non-significant; *$p < 0.05$. Each dot in the graphics represents a singular tumor and bars represent mean ± SEM.

mutation burden. As expected, our data revealed that, on average, the number of somatic variants observed in *VCMsh2*$^{LoxP/LoxP}$ tumors is significantly higher comparatively to *Apc*$^{Min/+}$ tumors. However, as we looked into the type of somatic mutation present in tumors from both models, we observed that, despite the significant high number of variants in *VCMsh2*$^{LoxP/LoxP}$ tumors, the profile of synonymous, non-synonymous and frameshift mutations was similar between the two models, with non-synonymous variants being the most frequent type of tumor-specific variants. These results are interesting and suggestive that independently of the cancer-associated molecular pathway underlying tumor formation, the pattern of mutation type is quite similar. In this aspect, the sum of protein-altering mutations, both non-synonymous and frameshifts, clearly surpasses the number of synonymous variants, indicating that those mutations have a role in neoplasia development. Summing up the exome data, tumors from the studied murine models follow the same trend found in human data, where MSI tumors harbor a higher mutation burden comparatively to MSS tumors[20].

The critical role that the immune response has in tumor onset and development is well known[33-38], and its understanding may contribute to improve the response to cancer immunotherapy[33]. It is known that CD8$^+$T cells are one of the most important agents in the anti-tumor immunity[3,39]. In HNPCC, due to the MSI phenotype, it has been postulated that the higher mutation burden and associated increased amount of neoantigens turns the tumor

cells more prone to lymphocyte recognition[40-42]. Particularly in MSI tumors, a marked presence of infiltrating cytotoxic CD8+ T cells can be observed[3,40]. In tumors from FAP patients, like in the majority of sporadic cancers which are microsatellite stable (MSS), the low mutational burden, and consequently low number of immunogenic neoantigens, is thought to hinder an effective immune response, allowing immune evasion[40]. Regarding T lymphocyte counts, we found that the murine models studied are comparable to human data, specifically in what refers to CD8+ cell infiltration[3,40]. In fact, we observed that the CD8+ infiltrate in *VCMsh2*$^{LoxP/LoxP}$ tumors is significantly higher comparatively to *Apc*$^{Min/+}$ tumors, supporting the role of CD8+ cytotoxic response as a key component of the host anti-tumoral immunity, particularly in tumors with the MSI phenotype. For CD4+ cells, we observed a tendency to a higher infiltrate in the *VCMsh2*$^{LoxP/LoxP}$ mice, though there was no statistically significant difference. Hence, these results show concordance with clinical data, in which MSI tumors are usually associated to higher numbers of infiltrating T lymphocytes, especially CD8+ cytotoxic cells.

With this study we conclude that these two mouse models studied in this work, *VCMsh2*$^{LoxP/LoxP}$ and *Apc*$^{Min/+}$, recapitulate the differences observed between HNPCC and FAP, either in terms of age of disease manifestation, incidence of intestinal tumors, mutation burden or lymphocyte infiltration. Therefore, results obtained with these preclinical mouse models are comparable with and translatable to the respective human scenario, demonstrating they are appropriate models to study and compare intestinal tumorigenesis. Moreover, due to recent evidence on the impact of gut microbiota on the development of CRC[43], we hypothesize these mice can also be suitable models to determine the mechanistic role of different microbes on the development of intestinal tumorigenesis, which can be addressed, for example, by altering microbiota composition.

Conflict of Interest

The authors declare no conflict of interest.

Ethics Statement

All mice were housed in the Animal Facility of Instituto de Investigação e Inovação em Saúde (i3S, University of Porto) and all procedures were performed according to the Ethics Committee and Direção Geral de Alimentação e Veterinária (DGAV) guidelines for care and use of laboratory animals.

Financial Support and Sponsorship

This research was funded (in part) by FCT - Fundação para a Ciência e a Tecnologia/Ministério da Ciência, Tecnologia e Ensino Superior in the framework of the projects "Financiamento Plurianual de Unidades de I&D, UIBD/04293/2020", by (in part) the project "P.CCC: Centro Compreensivo de Cancro do Porto" - NORTE-01-0145-FEDER-072678, supported by Norte Portugal Regional Operational Programme (NORTE 2020), under the PORTUGAL 2020 Partnership Agreement, through the European Regional Development Fund (ERDF), and (in part) by FCT project ref.:EXPL/MED-ONC/1592/2021.

REFERENCES

1. IJsselsteijn ME, Sanz-Pamplona R, Hermitte F, de Miranda NFCC. Colorectal cancer: A paradigmatic model for cancer immunology and immunotherapy. Mol Aspects Med 2019; 69: 123-129.
2. Bray F, Ferlay J, Soerjomataram I, Siegel RL, Torre LA, Jemal A. Global cancer statistics 2018: GLOBOCAN estimates of incidence and mortality worldwide for 36 cancers in 185 countries. CA Cancer J Clin 2018; 68: 394-424.
3. Deschoolmeester V, Baay M, Van Marck E, Weyler J, Vermeulen P, Lardon F, Vermorken JB. Tumor infiltrating lymphocytes: an intriguing player in the survival of colorectal cancer patients. BMC Immunol 2010; 11: 1-12.
4. Mauri G, Sartore-Bianchi A, Russo AG, Marsoni S, Bardelli A, Siena S. Early-onset colorectal cancer in young individuals. Mol Oncol 2019; 13: 109-131.
5. De Rosa M, Pace U, Rega D, Costabile V, Duraturo F, Izzo P, Delrion P. Genetics, diagnosis and management of colorectal cancer (Review). Oncol Rep 2015; 34: 1087-1096.

6. Pancione M, Remo A, Colantuoni V. Genetic and epigenetic events generate multiple pathways in colorectal cancer progression. Patholog Res Int 2012; 2012: 1-11.
7. Ewing I, Hurley JJ, Josephides E, Millar A. The molecular genetics of colorectal cancer. Frontline Gastroenterol 2014; 5: 26-30.
8. Rustgi AK. The genetics of hereditary colon cancer. Genes Dev 2007; 21: 2525-2538.
9. Mork ME, You YN, Ying J, Bannon SA; Lynch PM, Rodriguez-Bigas MA, Vilar E. High Prevalence of Hereditary Cancer Syndromes in Adolescents and Young Adults With Colorectal Cancer. J Clin Oncol 2015; 33: 3544-3549.
10. Pearlman R, Frankel WL, Swanson B, Zhao W, Yilmaz A, Miller K, Bacher J, Bigley C, Nelsen L, Goodfellow PJ, Goldberg RM, Paskett E, Shields PG, Freudenheim JL, Stanich PP, Lattimer I, Arnold M, Liyanarachchi S, Kalady M, Heald B, Greenwood C, Paquette I, Prues M, Draper DJ, Lindeman C, Kuebler JP, Reynolds K, Brell JM, Shaper AA, Mahesh S, Buie N, Weeman K, Shine K, Haut M, Edwards J, Bastola S, Wickham K, Khanduja KS, Zacks R, Pritchard CC, Shirts BH, Jacobson A, Allen B, se la Chapelle A, Hampel H. Prevalence and Spectrum of Germline Cancer Susceptibility Gene Mutations Among Patients With Early-Onset Colorectal Cancer. JAMA Oncol 2017; 3: 464-471.
11. Sinicrope FA. Lynch syndrome-associated colorectal cancer. N Engl J Med 2018; 379: 764–773.
12. Stoffel EM, Koeppe E, Everett J, Ulintz P, Kiel M, Osborne J, Williams L, Hanson K, Gruber SB, Rozek LS. Germline Genetic Features of Young Individuals With Colorectal Cancer. Gastroenterology 2018; 154: 897-905.
13. Ballester V, Rashtak S, Boardman L. Clinical and molecular features of young-onset colorectal cancer. World J Gastroenterol 2016; 22: 1736-1744.
14. Kucherlapati MH, Lee K, Nguyen AA, Clark AB, Hou Jr H, Rosulek A, Li H, Yang K, Lipkin M, Bronson RT, jelicks L, Kunkel TA, Kucherlapati R, Edelmann W. An Msh2 Conditional Knockout Mouse for Studying Intestinal Cancer and Testing Anticancer Agents. Gastroenterology 2010; 138: 993-1002.
15. Biller LH, Syngal S, Yurgelun MB. Recent advances in Lynch syndrome. Fam Cancer 2019; 18: 211-219.
16. Fishel R, Lescoe MK, Rao MR, Copeland NG, Jenkins NA, Garber J, Kane M, Kolodner R. The human mutator gene homolog MSH2 and its association with hereditary nonpolyposis colon cancer. Cell 1993; 75: 1027–1038.
17. Lothe RA, Peltomaki P, Meling GI, Aaltonen LA, Nystrom-Lahti M, Pylkkanen L, Heimdal K, Andersen TI, Moller P, Rognum TO. Genomic instability in colorectal cancer: relationship to clinicopathological variables and family history. Cancer Res 1993; 53: 5849–5852.
18. Marsischky GT, Filosi N, Kane MF, Kolodner R. Redundancy of Saccharomyces cerevisiae MSH3 and MSH6 in MSH2-dependent mismatch repair. Genes Dev 1996; 10: 407–420.
19. Brosens LA, Offerhaus GJ, Giardiello FM. Hereditary Colorectal Cancer: Genetics and Screening. Surg Clin North Am 2015; 95: 1067-1080.
20. Sahin IH, Akce M, Alese O, Shaib W, Lesinski GB, El-Rayes B, Wu C. Immune checkpoint inhibitors for the treatment of MSI-H/MMR-D colorectal cancer and a perspective on resistance mechanisms. Br J Cancer 2019; 121: 809-818.
21. Half E, Bercovich D, Rozen P. Familial adenomatous polyposis. Orphanet J Rare Dis 2009; 4: 1-23.
22. Kinzler KW, Vogelstein B. Lessons from hereditary colorectal cancer. Cell 1996; 87: 159–170.
23. Waller A, Findeis S, Lee MJ. Familial Adenomatous Polyposis. J Pediatr Genet 2016; 5: 78-83.
24. Yu H, Hemminki K. Genetic epidemiology of colorectal cancer and associated cancers. Mutagenesis 2020; 35: 207-219.
25. Aoki K, Taketo MM. Adenomatous polyposis coli (APC): a multi-functional tumor suppressor gene. J Cell Sci 2007; 120: 3327-3335.
26. Kwong LN, Dove WF. APC and its modifiers in colon cancer. Adv Exp Med Biol 2009; 656: 85-106.
27. Moser AR, Pitot HC, Dove WF. A Dominant Mutation that Predisposes to Multiple Intestinal Neoplasia in the Mouse. Science 1990; 247: 322-324.
28. Hanahan D. Dissecting multistep tumorigenesis in transgenic mice. Annu Rev Genet 1988; 22: 479-519.
29. Cory S, Adams JM. Transgenic mice and oncogenesis. Annu Rev Immunol. 1988; 6: 25-48.
30. Madison BB, Dunbar L, Qiao XT, Braunstein K, Braunstein E, Gumucio DL. Cis elements of the villin gene control expression in restricted domains of the vertical (crypt) and horizontal (duodenum, cecum) axes of the intestine. J Biol Chem 2002; 277: 33275-33283.
31. Su LK, Kinzler KW, Vogelstein B, Preisinger AC, Moser AR, Luongo C, Gould KA, Dove WF. Multiple intestinal neoplasia caused by a mutation in the murine homolog of the APC gene. Science 1992; 256: 668-670.
32. Jasperson KW, Tuohy TM, Neklason DW, Burt RW. Hereditary and familial colon cancer. Gastroenterology 2010; 138: 2044-2058.
33. Malka D, Lièvre A, André T, Taïeb J, Ducreux M, Bibeau F. Immune scores in colorectal cancer: Where are we?. Eur J Cancer 2020; 140: 105-118.
34. Haruki K, Kosumi K, Li P, Arima K, Vayrynen JP, Lau MC, Twombly TS, Hamada T, Glickman JN, Fujiyoshi K, Chen Y, Du C, Guo C, Vayrynen SA, Costa AD, Song M, Chan AT, Meyerhardt JA, Nishihara R, Fuchs CS, Liu L, Zhang X, Wu K, Giannakis M, Nowak JA, Ogino S. An integrated analysis of lymphocytic reaction, tumour molecular characteristics and patient survival in colorectal cancer. Br J Cancer 2020; 122: 1367-1377.
35. Giraldo NA, Sanchez-Salas R, Peske JD, Vano Y, Becht E, Petitprez F, Validire P, Ingels A, Cathelineau X, fridman WH, Sautés-Fridman C. The clinical role of the TME in solid cancer. Br J Cancer 2019; 120: 45-53.
36. Ogino S, Nowak JA, Hamada T, Phipps AI, Peters U, Milner Jr DA, Giovannucci EL, Nishihara R, Giannakis M, Garrett WS, Song M. Integrative analysis of exogenous, endogenous, tumour and immune factors for precision medicine. Gut 2018; 67: 1168-1180.

37. Gotwals P, Cameron S, Cipolletta D, Cremasco V, Crystal A, Hewes B, Mueller B, Quaratino S, Sabatos-Peyton C, Petruzzelli L, Engelman JA, Dranoff G. Prospects for combining targeted and conventional cancer therapy with immunotherapy. Nat Rev Cancer 2017; 17: 286-301.
38. Barnes TA, Amir E. HYPE or HOPE: the prognostic value of infiltrating immune cells in cancer. Br J Cancer 2017; 117: 451-460.
39. Titu LV, Monson JR, Greenman J. The role of CD8(+) T cells in immune responses to colorectal cancer. Cancer Immunol Immunother 2002; 51: 235-247.
40. Zaborowski AM, Winter DC, Lynch L. The therapeutic and prognostic implications of immunobiology in colorectal cancer: a review. Br J Cancer 2021; 125: 1341-1349.
41. Narayanan S, Kawaguchi T, Peng X, Qi Q, Liu S, Yan L, Takabe K. Tumor Infiltrating Lymphocytes and Macrophages Improve Survival in Microsatellite Unstable Colorectal Cancer. Sci Rep 2019; 9: 13455.
42. Green AR, Aleskandarany MA, Ali R, Hodgson EG, Atabani S, De Souza K, Rakha EA, Ellis IO, Madhusudan S. Clinical Impact of Tumor DNA Repair Expression and T-cell Infiltration in Breast Cancers. Cancer Immunol Res 2017; 5: 292-299.
43. Garret WS. Cancer and the microbiota. Science 2015; 348: 80-86.